Environmental Toxicology and Chemistry, 2025, **44(2)**, 363–374
https://doi.org/10.1093/etojnl/vgae036
Advance access publication: January 6, 2025
Original Article

Environmental Chemistry

Development of a bioaccumulation model for selenium oxyanions and organoselenium in stream biota

Adrian M. H. de Bruyn[1,*], Cybele B. Heddle[2], Jennifer Ings[3], Hakan Gürleyük[4], Kevin V. Brix[5,6], Samuel N. Luoma[7], and Mariah C. Arnold[2]

[1]ADEPT Environmental Sciences Ltd, Vancouver, BC, Canada
[2]Teck Coal Limited, Sparwood, BC, Canada
[3]Minnow Environmental, Georgetown, ON, Canada
[4]Brooks Applied Labs, Seattle, WA, United States
[5]EcoTox LLC, Miami, FL, United States
[6]Rosenstiel School of Marine, Atmospheric, and Earth Science, Marine Biology and Ecology, University of Miami, Miami, FL, United States
[7]Institute of the Environment, University of California, Davis, CA, United States

*Corresponding author: Adrian M. H. de Bruyn. Email: adrian.debruyn@outlook.com

Abstract

Selenium (Se) occurs in natural surface waters as a variety of inorganic and organic chemical species, typically dominated by the oxyanions selenate and selenite. Organoselenium species, although hypothesized to be more bioavailable than oxyanions, have rarely been identified or quantified in natural waters and little is known about their fate or bioaccumulative potential. We studied spatial patterns of bioaccumulation in relation to aqueous Se speciation over 5 years at more than 100 locations near coal mine operations in southeast British Columbia, Canada. We used a sequential approach to fitting bioaccumulation model coefficients, first using sites with no detectable organic Se species ($< 0.01\ \mu g\ L^{-1}$) to describe the bioaccumulation of selenate and selenite, then applying those relationships to the remaining sites to infer the bioavailability of detectable organoselenium species. Our analysis indicated that the methylated species methylseleninic acid was the most bioaccumulative form, followed by dimethylselenoxide. Organoselenium species were associated primarily with mine sedimentation ponds and are presumed to be products of Se metabolism by algae and bacteria. Highly bioavailable organoselenium species exported from the ponds appear to be responsible for enhanced Se bioaccumulation in biota in downstream lotic reaches, with this influence diminishing with distance from ponds as concentrations decline. Our findings indicate that managing biological productivity in mine sedimentation ponds could help manage Se risk in the receiving environment.

Keywords: selenium, speciation, bioaccumulation, mining

Introduction

Selenium (Se) speciation varies across different kinds of aquatic environments, affecting its fate (Milne, 1998; Maher et al., 2010), bioaccumulative potential (Riedel et al., 1991; Simmons & Wallschläger, 2005; Stewart et al., 2010), and toxicity (Besser et al., 1993; Janz et al., 2010). Selenium can occur in natural waters as the oxyanions selenate (SeO_4^{2-}, oxidation state +VI) and selenite (SeO_3^{2-}, oxidation state +IV), as elemental Se (oxidation state 0), and as organic or inorganic selenides (oxidation state -II). Selenate and selenite are thermodynamically stable and highly soluble in natural waters (Milne, 1998), although selenite is more reactive and has a tendency to adsorb to organic and mineral solid phases (Faust & Aly, 1981; Maher et al., 2010). Elemental Se is insoluble and generally occurs where microbial activity has resulted in the deposition of Se in solid phases (Dungan & Frankenberger Jr., 1999; Faust & Aly, 1981; Maher et al., 2010). Selenides and their degradation products have variable properties: some are soluble (e.g., seleninic acids), some are insoluble (e.g., metal selenides), and some are volatile (e.g., methylselenides). Early studies inferred that some forms of organoselenium were stable in natural waters based on the proportion of organoselenium relative to dissolved Se in oceans, estuaries, and larger rivers (Cutter & Bruland, 1984; Cutter & San Diego-McGlone, 1990). More recent studies in freshwaters, however, suggest that organoselenides are labile (LeBlanc & Wallschläger, 2016; Jain, 2017), perhaps due to a combination of metabolism, sequestration, and volatilization. For example, the amino acids selenomethionine (SeMet) and selenocysteine (SeCys) are ubiquitous in living systems but only their metabolites are detected in surface waters with any frequency (LeBlanc & Wallschläger, 2016). The complex biotic and abiotic processes that convert Se from one species to another have been reviewed elsewhere (Cutter & Bruland, 1984; Eswayah et al., 2016; Maher et al., 2010; Ponton et al., 2020).

Variation in Se speciation has been implicated in explaining patterns of Se bioaccumulation in different aquatic environments (e.g., Orr et al., 2006, 2012; Presser & Luoma, 2010; Stewart et al., 2010). In well-oxygenated lotic environments, selenate is often the dominant form of dissolved Se (Simmons & Wallschläger, 2005).

Received: April 13, 2024. **Revised:** September 30, 2024. **Accepted:** October 01, 2024

Conditions that favor the formation and retention of selenite and more reduced species such as organoselenium tend to be associated with the higher productivity and longer residence times of lentic environments (Orr et al., 2006, 2012; Presser & Luoma, 2010; Stewart et al., 2010). As a result, patterns of Se bioaccumulation in streams and rivers have been interpreted to mainly reflect the bioaccumulative potential of selenate, and the higher bioaccumulation sometimes observed in lakes and wetlands has been attributed to greater bioavailability of reduced forms of Se (Brix et al., 2005; Orr et al., 2006; Ponton et al., 2018; Ponton & Hare, 2013; Simmons & Wallschläger, 2005). This attribution has largely been inferential because Se speciation is not always determined in field studies and methods to identify and quantify organoselenium species are not widely available (Wallschläger & Feldmann, 2010; LeBlanc & Wallschläger, 2016).

Direct measurements of the bioaccumulative potential of Se species come from laboratory and mesocosm studies in which algae are exposed to individual Se species and then analyzed to measure net bioaccumulation. Such studies are subject to confounding factors such as depletion of Se in the growth medium and shifts in Se speciation during the study that are rarely measured (but cf Conley et al., 2011, 2013). These studies must be interpreted with caution because bioaccumulation can be attributed to the wrong Se species. Results of these studies can also be challenging to interpret in combination or in relation to field conditions because of differences among studies in factors such as algal growth rate, algal species or community composition, and composition of growth medium (Ponton et al., 2018). However, some general patterns have emerged. Most notably, laboratory studies have consistently reported that organoselenides are more bioaccumulative than oxyanions (Baines et al., 2001; Besser et al., 1993; Fournier et al., 2006; Kiffney & Knight, 1990; Ponton et al., 2018; Riedel et al., 1991). Unfortunately, most studies did not test environmentally relevant forms of organoselenium (LeBlanc & Wallschläger, 2016). Most investigators have tested SeMet, reporting bioaccumulation five- to 100-fold greater than selenite (Besser et al., 1993; Fournier et al., 2006; Kiffney & Knight, 1990; Ponton et al., 2018; Riedel et al., 1991). The bioaccumulative potential of other Se species is largely unknown, aside from a single study by Simmons and Wallschläger (2011) that reported "very little uptake" of selenocyanate (SeCN) by *Chlorella vulgaris*.

Few studies have attempted to directly link bioaccumulation of Se to aqueous Se speciation using field data. Ponton et al. (2018) found a correlation between Se concentrations in lake plankton and the sum of selenate and total dissolved organoselenium (inferred from measurements of selenite following UV conversion). Ponton et al. (2018) also reported large differences in bioaccumulation between natural lake microplankton and a monoculture of *Chlamydomonas reinhardtii* exposed to selenate, selenite, or SeMet in the laboratory. However, the authors were not able to identify or quantify organoselenium species in that study and thus could not confirm that speciation was stable during their exposures, making it challenging to quantitatively attribute bioaccumulation to particular Se species.

This study addresses two questions: to what degree can Se speciation explain patterns of bioaccumulation in a lotic food web, and how does bioavailability differ between Se species? We also attempted to identify where the most bioavailable forms of Se originated and compared their stability in streams in our study area. We resolved some of the challenges faced by previous studies by correlating observed bioaccumulation in the field to measured concentrations of individual inorganic and organic Se species related to coal mining. We applied liquid chromatography methods to quantify four inorganic and six organic Se species at parts-per-trillion levels in surface waters at 142 study sites over 5 years. The large number of samples ($n = 762$) and wide ranges of Se species concentrations in our dataset allowed sequential determination of model coefficients to assess the bioaccumulation of selenate, selenite, and detected organoselenium species in stream biota.

Methods

Study area

The Elk River watershed in southeast BC, Canada, is an area of historical and current metallurgical coal mining. The watershed contains reference areas unaffected by mining and areas with a range of mine-related effects on water quality. Monitoring has been conducted at dozens of sites throughout the watershed over more than a decade to evaluate Se bioaccumulation in benthic macroinvertebrates (BMIs) and other biota. Since 2018, there has also been an extensive monitoring program for aqueous Se speciation.

We described patterns of Se bioaccumulation in the field by combining data from field studies conducted between 2018 and 2022 at 142 lotic study sites, ranging from small streams directly receiving effluent from mine sedimentation and retention ponds ("mine ponds" hereafter) to the larger Fording and Elk rivers up to 75 km downstream. Sampling was conducted primarily in erosional riffles dominated by gravel-cobble substrate and consequently reflects a relatively simple food web dominated by biofilm, BMIs (predominantly Ephemeroptera, Plecoptera, and Trichoptera at most sites), and invertivorous fish. Thus, sampling focused on habitats where aqueous speciation in overlying waters is most likely to drive Se bioaccumulation in the food of the benthos, avoiding depositional areas and the ecological and biogeochemical complexity of Se dynamics that can occur in sediment (e.g., Martin et al., 2011, 2018, 2022). Because depositional characteristics can be ambiguous in the field, we reviewed field observations of flow, siltation, and the presence of BMI taxa characteristic of depositional environments (mainly Lumbriculidae, Gastropoda, and Odonata). Sites were classified according to evidence of depositional characteristics (See online supplementary material) and this classification was considered during model development to evaluate whether some sites might violate the lotic focus of the study.

Stream macroinvertebrate and water sampling and analysis

Because measurement of Se concentrations in basal food web resources can be confounded by inclusion of suspended particulates or mineral precipitates (Brandt et al., 2021; Hitchcock et al., 2009) and is subject to variability from short-term fluctuation in aqueous [Se], speciation, and growth conditions (Brandt et al., 2021; DeForest et al., 2016), monitoring in our study area uses BMI [Se] as a pragmatic and reliable measure of Se bioaccumulation. We interpret BMI [Se] to reflect uptake of aqueous Se species by primary producers followed by trophic transfer to BMIs, noting that direct uptake from the aqueous phase is a minor contributor to Se concentrations in consumers (Stewart et al., 2010).

Macroinvertebrate tissue was collected as replicate composite grab samples by kick-and-sweep methods following Canadian Aquatic Biomonitoring Network protocols (Environment Canada, 2012). Samples were collected by moving across the stream channel from bank to bank in an upstream direction with a triangular net (36-cm sides, 400-μm mesh) held immediately downstream of the sampler's feet. Organisms were removed using forceps to obtain > 0.5 g wet tissue with composition approximating relative abundances of BMI taxa in the net. Samples were photographed,

placed into sterile 20-mL scintillation vials in a cooler with ice packs, transferred to a freezer, and shipped frozen by courier to the analytical laboratory. Total Se analysis was conducted at the Saskatchewan Research Council (Saskatoon, SK, Canada) using double quadrupole inductively coupled plasma mass spectrometry (ICP-MS) of nitric acid digested dry samples or by TrichAnalytics Inc. (Saanichton, BC, Canada) using laser ablation ICP-MS of dry pelletized samples. Both laboratories use industry standard quality assurance and quality control measures, including analysis of certified reference materials, and in all cases confirmed that data quality objectives were met. Ashby et al. (2023) provide a detailed analysis of data quality for these analytical methods. Replicate results from each sampling event were averaged prior to modelling to avoid pseudoreplication.

Water samples were collected in most cases concurrently and always within 1 week of tissue samples by wading in an upstream direction into a midchannel area and inverting sample bottles at middepth. Water samples for speciation analysis were filtered (0.45 µm) at the time of collection and frozen until analysis to minimize changes to speciation through biological or chemical reactions. Sample fractions for volatile species analysis (see *Se speciation analysis* section) were stabilized with an organic solvent in the field and refrigerated prior to analysis. Total Se, dissolved Se, and sulphate were measured by ALS Environmental (Calgary, AB, Canada) using ICP-MS.

Se speciation analysis

Speciation analysis was conducted by Brooks Applied Labs (Seattle, WA, USA). All samples were analyzed for selenate, selenite, dimethylselenoxide (DMSeO), methylseleninic acid (MeSe(IV)), methaneselenonic acid (MeSe(VI)), selenocyanate, selenosulphate ($SeSO_3$), and SeMet using ion chromatography inductively coupled plasma collision reaction cell mass spectrometry (IC-ICP-CRC-MS). Selenium species were chromatographically separated on an ion exchange column, similar to the conditions described in Wallschläger and Bloom (2001) but with modifications to the gradient to facilitate baseline separation of the target organoselenium species. Eluted species were then quantified using an ICP-MS equipped with a collision reaction cell for effective removal of polyatomic interferences. Selected samples ($n = 186$) were also analyzed for the volatile species dimethylselenide (DMSe) and dimethyldiselenide (DMDSe) using reversed-phase liquid chromatography coupled to ICP-CRC-MS (similar to Lunøe et al., 2010). Species identification and quantitation for both methods were accomplished by analysis of known standards of the listed Se species. Quality control for each set of samples included method blanks, sample duplicates, and fortified (spiked) samples. Fortified samples and calibration curves were prepared using the same source standards, and independent second-source standards were used to verify the accuracy of the calibration curves. Instrument calibration and species retention times were verified every 10 samples.

Bioaccumulation analysis

Our approach to bioaccumulation analysis modeled each individual Se species as an additive contributor to total BMI [Se]. Like nearly all previous empirical modelling studies (e.g., Presser & Luoma, 2010; but cf, e.g., DeForest et al., 2016; Brandt et al., 2021), this approach implicitly assumes that Se exposure of the food web reflects simultaneously measured local conditions. Antecedent exposures (e.g., Brandt et al., 2021) and lags (e.g., Beckon, 2016) are not taken into account. However, our approach differs from most previous analyses in two important ways. First, most previous work modeled bioaccumulation as a function of aqueous total or dissolved [Se], with effects of variable (uncharacterized) speciation producing residual variance and nonlinearity (e.g., Brix et al., 2005; Orr et al., 2012; Kuchapski & Rasmussen, 2015; DeForest et al., 2017; but cf Vriens et al., 2016; Ponton et al., 2018). By explicitly describing the contribution to bioaccumulation from each species, we sought to develop a model that would explain and predict bioaccumulation across a range of speciation conditions. Second, other models fit separate functions for uptake of total Se from water into basal resources and trophic transfer from basal resources into BMIs (e.g., Presser & Luoma, 2010; but cf, e.g., Brix et al., 2005; Ponton & Hare, 2013). By modeling the combined outcome of these two processes using Se measurements in BMIs, our analysis avoids several sources of sampling and analytical uncertainty that affect Se measurements in basal resources (see Stream macroinvertebrate and water sampling and analysis section). Macroinvertebrate [Se] provides a relatively unconfounded measure of bioaccumulation (Brandt et al., 2021), which improved our ability to quantify the contribution of individual Se species.

The model form used in our analysis (description and rationale follows) was:

$$[Se]_{BMI} = [SeVI]\left(a_{Se(VI)}[Se(VI)]^{b_{Se(VI)}}[SO_4]^{b_{SO4}}\right) + [Se(IV)]\left(a_{Se(IV)}[Se(IV)]^{b_{Se(IV)}}\right) + [DMSeO](a_{DMSeO}) + [MeSe(IV)]\left(a_{MeSe(IV)}\right) \quad \text{(Eq. 1)}$$

where $[Se]_{BMI}$ is BMI [Se] (mg kg^{-1} dry weight); [Se(VI)] is selenate concentration (µg L^{-1}); $[SO_4]$ is sulphate concentration (mg L^{-1}); [Se(IV)] is selenite concentration (µg L^{-1}); [DMSeO] is DMSeO concentration (µg L^{-1}); and [MeSe(IV)] is MeSe(IV) concentration (µg L^{-1}). Formulating the model in this way facilitates calculation of bioaccumulation factors for each Se species using the terms in round brackets (multiplied by 1,000 µg mg^{-1} to reconcile units). To facilitate comparing our results with other studies, we converted bioaccumulation factors into estimated algae-water concentration ratios (known as the enrichment factor [EF] sensu Stewart et al., 2010, or the operational distribution coefficient [K_d] sensu Presser & Luoma, 2010) by dividing the BMI bioaccumulation factor by a mean trophic transfer factor of 2.8 (Presser & Luoma, 2010). For all analyses described below, both sides of the equation were log_{10}-transformed to stabilize residual variance prior to estimating model coefficients using the nonlinear regression function of Systat 13.2 (Inpixon, Palo Alto, CA, USA).

Uptake of individual Se species was modeled by taking a sequential approach to fitting coefficients, thereby reducing potential variance inflation caused by multicollinearity among species. Bioaccumulation model coefficients were first fit using cases in which selenate was the only detected Se species. This initial analysis included only the selenate (first) group of terms in *Equation 1*, with other terms assumed to be zero. The selenate group included coefficients for concentration dependence (Bailey et al., 1995; Lo et al., 2015) and sulphate dependence (Bailey et al., 1995; Lo et al., 2015; Ponton et al., 2018; Riedel & Sanders, 1996; Williams et al., 1994) of selenate bioaccumulation. The coefficient $b_{Se(VI)}$ describes the dependence of selenate uptake on [Se(VI)]: $b_{Se(VI)} = 0$ would indicate that selenate uptake is linear to [Se(VI)], whereas a negative value for $b_{Se(VI)}$ would indicate that selenate uptake is less-than-linear to [Se(VI)]. The coefficient b_{SO4} describes the inhibition of selenate uptake by sulphate: b_{SO4}=0 would indicate no inhibition, whereas a negative value

for b_{SO4} would indicate that selenate uptake declines with increasing [SO_4].

After fitting model parameters for selenate, the analysis was repeated using cases in which selenite was detected but there were no detectable organoselenium species (< 0.01 µg L^{-1}). This second analysis included the selenate (first) and selenite (second) groups of terms in *Equation 1*, with a coefficient for concentration dependence of selenite bioaccumulation ($b_{Se(IV)}$); Besser et al., 1993; Riedel & Cole, 2001; Swift, 2002; Conley et al., 2009, 2011, 2013; DeForest et al., 2016). The coefficient $b_{Se(IV)}$ describes the dependence of selenite uptake on [Se(IV)]: $b_{Se(IV)} = 0$ would indicate that selenite uptake is linear to [Se(IV)], whereas a negative value for $b_{Se(IV)}$ would indicate that selenite uptake is less-than-linear to [Se(IV)]. Parameters for selenate ($a_{Se(VI)}$, $b_{Se(VI)}$, b_{SO4}) were fixed at the values estimated in the previous step and new model parameters ($a_{Se(IV)}$, $b_{Se(IV)}$) were estimated for selenite.

Finally, the model form used in the oxyanion-only analysis was expanded again to include the organoselenium (third and fourth) terms in *Equation 1*. Parameters for selenate and selenite were fixed at the values estimated above and new parameters were estimated using data from samples with detectable organoselenium (≥ 0.01 µg L^{-1}). Model terms for frequently detected organoselenium species were initially evaluated with coefficients for concentration dependence, but these coefficients were not significant and were not retained. Potential concentration dependence of organoselenium bioaccumulation was evaluated further by inspection of residuals of the adopted model form with concentration-independent terms.

We conducted a preliminary analysis that included all samples in our dataset ($n = 826$) and noted some samples that did not conform well to the prevailing pattern (See online supplementary material Figures S2 and S3). We explored the hypothesis that these samples were from depositional areas by testing whether model residuals differed between sites classified on the basis of visible siltation and presence of depositional BMI taxa (See online supplementary material Figure S4). Analysis of variance and post hoc comparisons using Tukey's honestly significant difference identified five sites with depositional characteristics that had significantly higher model residuals than the 137 nondepositional sites (results provided in the online supplementary material). We hypothesize that fine sediments at the depositional sites facilitate anaerobic microbial processing of Se and the development of more reduced porewater speciation that differs from what is measured in the overlying water (Martin et al., 2011, 2018, 2022). Under such conditions, local porewaters are likely to influence exposures of the food web, confounding the link between BMI [Se] and measured Se speciation in overlying water. We therefore reparametrized our model after removing these five sites from the dataset as not representative of the direct exposure pathway, leaving $n = 762$ from 137 sites. Thus, the model we present describes Se bioaccumulation in biota from nondepositional lotic environments, taking advantage of Se speciation changes occurring in upstream lentic environments while minimizing local influences such as porewater speciation changes and variable BMI composition that are characteristic of lentic areas.

Model evaluation and sensitivity analysis

Models were evaluated using the mean-corrected coefficient of determination (r^2_{corr}), ratio of parameter to asymptotic standard error (P/ASE), 95% confidence interval (CI) of estimated parameters, agreement factor (AF), and residuals. Mean-corrected sums of squares are calculated after subtracting the grand mean of the dependent variable from each observation, and the r^2_{corr} calculated from these sums of squares is considered to better reflect how much variance is truly explained by a nonlinear regression model compared with a raw r^2. The ratio of an estimated parameter to its ASE can be roughly read as a *t*-statistic, providing similar information about the precision of the estimate. Agreement factor is the proportion of observations that are within a specified factor (herein, factors of 1.5 and 2) of model predictions. Overall performance of the oxyanion-only terms in the model was evaluated using AF and inspection of residuals when applied to the full dataset with no detected organoselenium ($n = 463$). Overall performance of the full model with terms for selenate, selenite, MeSe(IV), and DMSeO was evaluated using AF and inspection of residuals when applied to the full final dataset ($n = 762$).

Results and discussion

Patterns of Se speciation

The final dataset comprised 762 sampling events from 12 reference sites unaffected by mining (total [Se] 0.16–1.88 µg L^{-1}; BMI [Se] 2.7–10.3 mg kg^{-1} dry wt) and 125 sites downstream of mining (total [Se] 0.15–401 µg L^{-1}; BMI [Se] 1.4–115 mg kg^{-1} dry wt). Data used in each step of the sequential modelling analysis are summarized in Table 1. All data used in our analyses are provided in online supplementary material.

The two frequently detected organoselenium species in our dataset were MeSe(IV; 283 detections in 762 analyses; 0.010–0.676 µg L^{-1}) and DMSeO (96 detections in 762 analyses; 0.010–0.434 µg L^{-1}). Three additional organoselenium species were detected at a lower frequency in our dataset. MeSe(VI; 38 detections in 694 analyses; 0.012–0.135 µg L^{-1}) was occasionally detected in a 1 km stream reach downstream of a water treatment facility, where it appears to be generated by an oxidation treatment step designed to convert reduced Se species into selenate, and in a single sample collected downstream of a mine pond. The volatile species DMDSe (four detections in 186 analyses; 0.026–0.144 µg L^{-1}) and DMSe (26 detections in 186 analyses; 0.026–0.446 µg L^{-1}) were detected infrequently and only in samples collected immediately downstream of certain mine ponds. Additional model runs were conducted to estimate coefficients for these species, but regression analysis was unable to detect an effect on bioaccumulation of MeSe(VI), DMSe, or DMDSe. Selenocyanate and $SeSO_3$ were rarely detected at our study sites ([SeCN] 0.011–0.020 µg L^{-1}, six detections in 784 analyses; [$SeSO_3$] 0.011–0.027 µg L^{-1}, four detections in 784 analyses) and are expected to have negligible bioavailability (Simmons & Wallschläger, 2011). Selenomethionine, although known to be

Table 1. Datasets used to derive the selenium (Se) bioaccumulation model.

Parameter	Modeling step		
	1: Se(VI)	2: Se(IV)	3: Organoselenium
n	78	397	287
BMI [Se] (mg kg^{-1} dry wt)	3.0–10.2	1.4–21.0	1.9–115
[Se(VI)] (µg L^{-1})	0.16–151	0.15–252	0.05–401
[SO_4] (mg L^{-1})	6–815	4.9–1760	30.4–1420
[Se(IV)] (µg L^{-1})	<0.010	0.011–0.706	0.069–6.33
[MeSe(IV)] (µg L^{-1})	<0.010	<0.010	<0.01–0.676
[DMSeO] (µg L^{-1})	<0.010	<0.010	<0.01–0.434
[MeSe(VI)] (µg L^{-1})	<0.010	<0.010	<0.01–0.135
[DMSe] (µg L^{-1})	<0.022	<0.022	<0.022–0.446
[DMDSE] (µg L^{-1})	<0.022	<0.022	<0.022–0.144

Note. BMI [Se] = benthic macroinvertebrate selenium concentration; Se(VI) = selenate; SO4 = sulphate; Se(IV) = selenite; MeSe(IV) = methylseleninic acid; DMSeO = dimethylselenoxide; MeSe(VI) = methane selenonic acid; DMSe = dimethylselenide; DMDSe = dimethyldiselenide.

highly bioavailable (Besser et al., 1993; Fournier et al., 2006; Kiffney & Knight, 1990; Ponton et al., 2018; Riedel et al., 1991), was not detected in any sample.

The first novel finding from our field study is that effluent from mine ponds can expose downstream lotic areas to concentrations of selenite up to 6 µg L^{-1} and methylated selenides up to nearly 1 µg L^{-1} (Figure 1), with significant implications for Se bioaccumulation (see *Patterns of Se bioaccumulation* section). The highest concentrations of reduced species can be attributed to the passage of mine-influenced water through some (but not all) mine ponds. Whereas selenate concentrations were broadly similar upstream and immediately downstream of mine ponds (Figure 1A), selenite exhibited a 3.6-fold increase in median concentrations and a 4.6-fold increase in maximum concentrations (Figure 1B) downstream versus upstream of these ponds. Similarly, maximum [MeSe(IV)] increased 12.5-fold (Figure 1C)

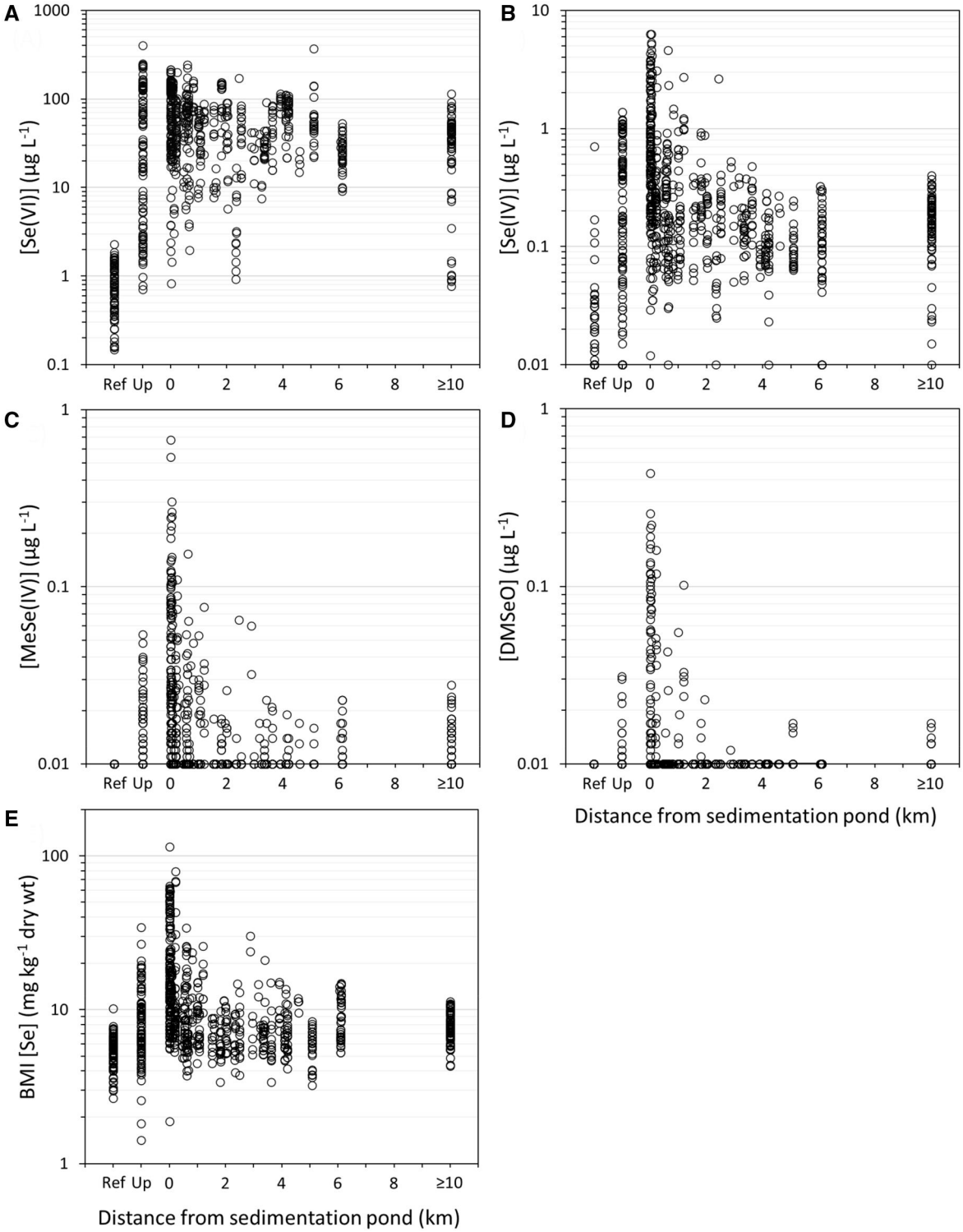

Figure 1. Spatial distribution of (A) selenate [Se(VI)], (B) selenite [Se(IV)], (C) methylseleninic acid [MeSe(IV)], (D) dimethylselenoxide [DMSeO], and (E) benthic macroinvertebrate selenium concentration (BMI [Se]) relative to constructed mine ponds. Ref denotes reference sites with no upstream mining. Up denotes sites with mining influence but upstream of mine ponds. Symbols on the x-axis are non-detects.

and maximum [DMSeO] increased 7.9-fold downstream versus upstream (Figure 1D). The bioavailability of reduced Se species was apparent in a 3.4-fold increase in maximum BMI [Se] downstream versus upstream (Figure 1E).

Study sites further downstream of mine ponds exhibited a gradual decline in selenate concentrations of about 50% within 10 km, reflecting progressive dilution as tributaries flow into larger rivers (Figure 1A). Selenite and MeSe(IV) exhibited steeper declines with distance, indicating greater bioavailability and/or lability than selenate, but were still detectable at some sites ≥ 10 km downstream. Dimethylselenoxide exhibited the steepest decline with distance and was rarely detected beyond 2 km. Zhang et al. (2014) found similarly steep declines in concentrations of reduced Se species with distance from mines in China. The wide ranges of concentrations apparent in Figure 1 provided an opportunity to study how individual Se species contributed to bioaccumulation.

The occurrence of DMSeO and MeSe(IV) downstream of mine ponds indicates that conditions in these ponds promote biological Se metabolism, including pathways that result in formation of volatile methylated species. Dimethylselenoxide and MeSe(IV) are oxidation products of the volatile species DMSe and DMDSe (Goeger & Ganther, 1994; Rosenfeld et al., 2020; Wang & Burau, 1995; Winkel et al., 2010; Zhang et al., 1999), which are secondary metabolites of assimilatory reduction of Se by algae and bacteria (Cooke & Bruland, 1987; Eswayah et al., 2016; Ponton et al., 2020; Zhang & Frankenberger Jr., 2000). LeBlanc and Wallschläger (2016) detected MeSe(IV) in the medium of a culture of *Chlorella vulgaris* exposed to selenate, noting that MeSe(IV), DMSe, and DMDSe are all known oxidation products of methylated SeCys, which is a metabolite of SeMet.

Conditions that promote the formation of volatile methylated Se (and thus would promote the formation of MeSe(IV) and DMSeO) have most often been studied in the context of bioremediation of Se by constructed wetlands. In general, Se methylation in wetlands is reported to be a relatively slow and inefficient process (See review by Neumann et al., 2003). In contrast, Neumann et al. (2003) reported rapid conversion of selenate to DMSe by *Chlorella* sp. in the absence of sulphate, occurring at rates orders of magnitude higher than have been reported in natural wetlands. Similarly high conversion rates were not observed for macroalgae (*Chara* and *Enteromorpha*). Algae in that study converted 90% of supplied selenate to selenoamino acids, which were then converted to DMSe. Neumann et al. (2003) further reported that conversion of selenate to DMSe over a 20-hr experiment was strongly inhibited by sulphate (inferred to inhibit selenate uptake) but was not affected by addition of nitrate, treatment with penicillin (ruling out bacterial contamination as a source), or incubation in the dark (indicating that photosynthesis was not required for DMSe production under these conditions).

The conditions that promote biological Se metabolism in mine ponds may be similar to those that enhance Se bioaccumulation in natural lentic areas. Many of the studied ponds have visible growth of unicellular and colonial algae and abundant aquatic macrophytes that provide well-lit surface area for ephiphytic production and enhance delivery of organic detritus to sediment. Mine ponds are designed to enhance settling and retention of particulate matter, which would increase the potential for suboxic conditions in sediment and thereby promote anaerobic Se reduction (Martin et al., 2011, 2018, 2022). Some mine ponds in our study area also have geosynthetic liners and/or baffles, which are usually black and therefore provide warm, well-lit surfaces for biofilm production. However, mine ponds are also designed to be flow-through systems, which facilitates the export of biologically generated organoselenium to the downstream lotic areas that were the focus of our study.

Patterns of Se bioaccumulation

The relationship between BMI [Se] and aqueous total [Se] (Figure 2) resembled the segmented regression relationships described in some previous models (e.g., Adams et al., 2003; Brix et al., 2005). However, the appearance of two stages of bioaccumulation in our dataset (and possibly in the datasets of previous studies) is an artifact of uneven occurrence of highly bioavailable organoselenium species along the studied gradient of aqueous Se (Figure 2). A more informative and generalizable model can be obtained by explicit consideration of the unequal bioavailability of different Se species.

Sites at which only selenate was detected exhibited low Se bioavailability, with BMI [Se] increasing from 5.1 to 6.5 mg kg^{-1} dry weight as aqueous total [Se] increased from 0.16 µg L^{-1} to 151 µg L^{-1} (Figure 2). Sites at which both selenate and selenite were detected (but with no detectable organoselenium) exhibited greater variability and a slightly steeper increase in BMI [Se] to the selenate-only sites (Figure 2). The similarity of bioaccumulation relationships for these two subsets of data indicates that the concentrations of selenite at these sites (≤ 0.7 µg L^{-1}) caused a small (< 2 mg kg^{-1} dry wt) increment in BMI [Se] relative to the effect of selenate.

Low bioavailability of Se in lotic areas was also reported by Orr et al. (2012) and Kuchapski and Rasmussen (2015), who described patterns of bioaccumulation similar to those observed in our study (black lines on Figure 2). In a review of data from many studies, Presser and Luoma (2010) summarized experimental EFs of 140–493 when selenate was the dominant form and 720–2,800 when selenite was elevated across a range of water quality conditions. Ponton et al. (2020) reported a wide range of field-derived

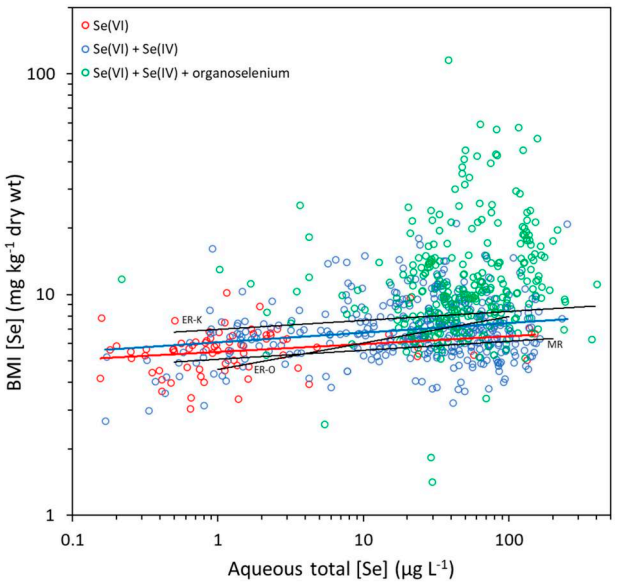

Figure 2. Selenium (Se) concentrations in benthic macroinvertebrates (BMIs) relative to aqueous total Se at study sites with differing speciation. Red symbols and line are sites where only selenate (Se(VI)) was detected; blue symbols and line are sites where both Se(VI) and selenite (Se(IV)) were detected. Green symbols (no line shown) are sites with detectable Se(VI), Se(IV), and organoselenium. Black lines are lotic bioaccumulation models derived by Orr et al. (2012) for the Elk River (ER-O) and Kuchapski and Rasmussen (2015) for the Elk River (ER-K) and McLeod River (MR).

EFs from lotic fresh waters, ranging from 12,000 at total [Se] near 0.1 µg L^{-1} to 50 at total [Se] near 30 µg L^{-1}. The data shown in Figure 2 indicate a range of field-derived EFs from near 2,000 at 1 µg L^{-1} total [Se] to near 20 at 100 µg L^{-1} total [Se], consistent with overall selenate-dominated conditions and a range of influence from selenite (Presser and Luoma, 2010). Observed EFs at the high end of the range of total [Se] were lower than the ranges summarized by Presser and Luoma (2010) and Ponton et al. (2020), indicating a negative relationship between EF and selenate (Bailey et al., 1995; Lo et al., 2015) and sulphate concentrations in our study area (Bailey et al., 1995; Lo et al., 2015; Ponton et al., 2018; Riedel & Sanders, 1996; Williams et al., 1994). Sulphate concentrations were typically > 500 mg L^{-1} at sites in our study area with total [Se] > 100 µg L^{-1} (Table 1).

Sites at which organoselenium was detected exhibited the greatest variability in BMI [Se] and an increment in bioaccumulation relative to sites with only oxyanions (Figure 2). These sites most frequently occurred at aqueous total [Se] > 20 µg L^{-1}, reflecting stream reaches most influenced by mine effluent discharged via mine ponds. Organoselenium was rarely detected at sites in larger rivers. Nearly all sites with detectable organoselenium (> 0.01 µg L^{-1}) exhibited BMI [Se] greater than the mean at sites with no detectable organoselenium (Figure 2). The highest BMI [Se] (up to 115 mg kg^{-1} dry wt) occurred at sites with organoselenium concentrations between 0.5 and 1 µg L^{-1}.

Bioaccumulation model coefficients for oxyanions

Analysis of selenate-only cases (Table 1) gave model coefficients of –0.936 for selenate dependence and –0.052 for sulphate dependence (Table 2). These coefficients indicate that selenate uptake does not increase in direct proportion to aqueous selenate and is inhibited by sulphate (because both are negative). Selenate uptake appears almost completely saturated across the studied range of aqueous selenate concentrations (because $b_{Se(VI)}$ is near –1), resulting in very little change in BMI [Se] across a wide range of [Se(VI)] (see also Figure S5). We note that collinearity of selenate and sulphate concentrations in our field dataset (Figure S1) may have affected the fitted coefficients for these parameters. However, model residuals were homoscedastic and unstructured with respect to concentrations of either selenate or sulphate (See online supplementary material Figure S6), supporting the selected model form.

The selenate dependence coefficient had a large |P/ASE| and a CI that excluded zero (Table 2), indicating that the estimated value is likely robust. The value estimated by our analysis ($b_{Se(VI)} = -0.936$) implies stronger saturation of selenate uptake than previous estimates derived from a compilation of data from multiple laboratory and field studies ($b_{Se(VI)} = -0.591$ [DeForest et al., 2017]) and from laboratory studies with *Chlamydomonas reinhardtii* ($b_{Se(VI)} = -0.492$ [estimated from Riedel & Sanders, 1996]) and *Raphidocelis subcapitata* ($b_{Se(VI)} = -0.315$ [estimated from Lo et al., 2015]). The selenate coefficient may have been over-estimated by misattribution of variance due to sulphate (Figure S1). Alternatively, stronger saturation in our field dataset versus laboratory studies may relate to the more complex assemblage of species (natural biofilm communities vs. monocultures of Chlorophyta) or the wider range of selenate concentrations in our field dataset (0.16–151 µg L^{-1} vs. 3–10 µg L^{-1} [Riedel & Sanders, 1996] or 5–40 µg L^{-1} [Lo et al., 2015]).

The sulphate dependence coefficient ($b_{SO4} = -0.052$) had |P/ASE| near 1 and a CI that did not exclude zero (Table 2), indicating that this estimate is imprecise and evidence for sulphate inhibition of selenate uptake is equivocal in this dataset. Based on strong evidence that sulphate inhibits selenate uptake in experimental exposures (Bailey et al., 1995; Lo et al., 2015; Ponton et al., 2018; Riedel & Sanders, 1996; Williams et al., 1994), we retained the sulphate dependence term in our model. Studies with laboratory monocultures have shown a stronger effect of sulphate on selenate uptake, with larger negative coefficients for *C. reinhardtii* ($b_{SO4} = -0.282$ [estimated from Riedel & Sanders, 1996]; $b_{SO4} = -0.714$ [estimated from Ponton et al., 2018]) and *R. subcapitata* and *Lemna minor* ($b_{SO4} = -0.568$ [calculated by DeForest et al., 2017 from data in Lo et al., 2015]). As discussed above, collinearity between independent variables may have led to under-estimation of the sulphate coefficient. However, Ponton et al. (2018) reported selenate uptake data for field-collected microplankton that exhibited a sulphate dependence coefficient of –0.117, which is within the CI of our estimate (95% CI: –0.134–0.030). The wide variance among studies cited above suggests that there may be important effects of algal species or other factors that differ between laboratory and field studies. In addition, the effect of sulphate could become weaker when uptake sites are saturated by very high sulphate concentrations (Ponton et al., 2020).

Fixing the model parameters for selenate at the values in Table 2 and rerunning the analysis on cases with detectable selenite (but no detectable organoselenium; Table 1) gave an estimated model coefficient of –0.373 for selenite dependence (Table 2). This coefficient had |P/ASE| near 2 and a CI that did not exclude zero, indicating that this estimate is imprecise and evidence for selenite concentration dependence is equivocal in this dataset. However, our estimated coefficient was close to values estimated using data from experimental studies with *C. reinhardtii* ($b_{Se(IV)} = -0.329$ [Besser et al., 1993]), mixed periphyton cultures ($b_{Se(IV)} = -0.258$ [Conley et al., 2011]), and pooled BMIs in stream mesocosms ($b_{Se(IV)} = -0.196$ [Swift, 2002]).

The parameter estimates in Table 2 indicate greater bioavailability of selenite in our study area (typically 0.1–1 µg L^{-1}, giving EF = 1128–2661) compared with selenate (typically 1–100 µg L^{-1}, giving EF = 25–1844 at 100 mg L^{-1} SO_4). However, the relative bioavailability of these species depends on concentration and effects of sulphate. The model predicts that selenate bioavailability can exceed that of selenite when selenate and sulphate concentrations are low (e.g., 0.1 µg L^{-1} selenate and 10 mg L^{-1} SO_4 gives EF = 17,942) or selenite concentrations are high (e.g., 10 µg L^{-1} selenite gives EF = 478). Concentration and sulphate dependence of EF explains why some studies have reported higher bioavailability of selenate (Fournier et al., 2006; Neumann et al., 2003; Simmons & Wallschläger, 2011), some have reported similar bioavailability or inconsistent results (Conley et al., 2013; Ponton et al., 2018), and some have reported higher bioavailability of

Table 2. Estimated parameters of the selenium bioaccumulation model.

Species	Parameter	Estimate (95% CI)	P/ASE	Predicted EF
Selenate	$a_{Se(VI)}$	6.56 L g^{-1} (4.68, 8.45)	6.94	25–1844[a]
	$b_{Se(VI)}$	−0.936 (−0.993, −0.879)	−32.7	
	b_{SO4}	−0.052 (−0.134, 0.030)	−1.26	
Selenite	$a_{Se(IV)}$	3.16 L g^{-1} (0.829, 5.48)	2.66	1127–2661[b]
	$b_{Se(IV)}$	−0.373 (−0.758, 0.012)	−1.90	
DMSeO	a_{DMSeO}	13.1 L g^{-1} (−13.4, 39.5)	0.970	4671
MeSe(IV)	$a_{MeSe(IV)}$	104 L g^{-1} (84.2, 124)	10.3	37146

Note. CI = confidence interval; EF = enrichment factor; P/ASE = ratio of parameter estimate to asymptotic standard error; DMSeO = dimethylselenoxide; MeSe(IV) = methylseleninic acid; Se(VI) = selenate; Se(IV) = selenite.
[a] Range shown for 1–100 µg L^{-1} selenate at 100 mg L^{-1} sulphate.
[b] Range shown for 0.1–1 µg L^{-1} selenite.

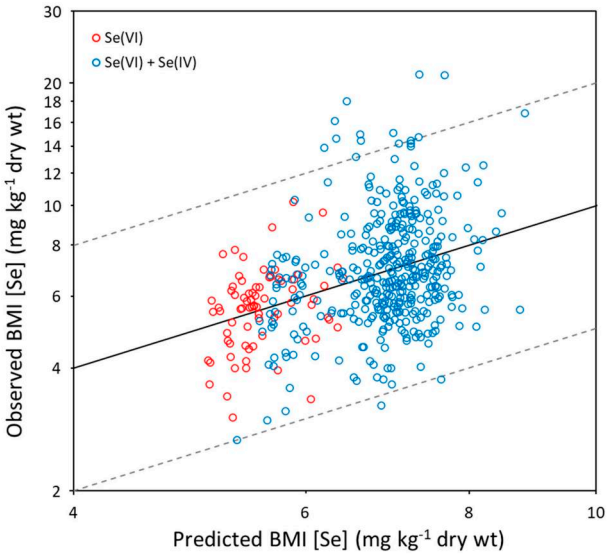

Figure 3. Overall performance of model terms for selenium (Se) oxyanions. Solid diagonal line is perfect agreement between observed and predicted benthic macroinvertebrate (BMI) Se concentrations. Dashed diagonal lines indicate plus or minus a factor of 2 from perfect agreement. Se(VI) = selenate; Se(IV) = selenite.

selenite (Hu et al., 1997; Luoma & Rainbow, 2008; Vriens et al., 2016).

The model fit to selenate-only cases had an r^2_{corr} of 0.076, reflecting the low bioaccumulation of selenate in our study area and resulting shallow relationship apparent on Figure 2. Addition of a selenite term increased r^2_{corr} to 0.14 and increased the slope of the bioaccumulation relationship only slightly (Figure 2). Model residuals were homoscedastic within each dataset and did not vary systematically with concentrations of either oxyanion (See online supplementary material Figure S7), supporting the selected model form with concentration dependence of both oxyanions. Despite the relatively low influence of Se oxyanion concentrations on BMI [Se], 84% of observations were within a factor of 1.5 of model predictions and 96% were within a factor of 2 (Figure 3). Potential sources of this residual variance are discussed below (see *Summary* section).

Bioaccumulation model coefficients for organoselenium

Analysis of cases with one or more detectable organoselenium species gave estimated coefficients of 13.1 for DMSeO and 104 for MeSe(IV) (Table 2). The DMSeO coefficient had |P/ASE| <1 and a CI that did not exclude zero, indicating that the estimated value is imprecise and evidence for bioaccumulation of DMSeO is equivocal in this dataset. The MeSe(IV) coefficient had a relatively large |P/ASE| and a CI that excluded zero, indicating that the estimated value is likely robust. These coefficients give estimated EFs of 4,671 (95% CI: 0–14123) for DMSeO and 37,146 (95% CI: 30,065–44,227) for MeSe(IV). These EFs are similar to (DMSeO) or substantially higher than (MeSe[IV]) the value of 4,000 estimated from a relationship between [Se] in *Chaoborus* and aqueous organoselenium (Ponton & Hare, 2013).

The model fit to the full dataset had an r^2_{corr} of 0.52. Model residuals were homoscedastic and did not vary systematically with concentrations of either organoselenium species (Figure 4), supporting the selected model form without concentration dependence for organoselenium. Performance of the full model applied to the full dataset was comparable to the oxyanion-only

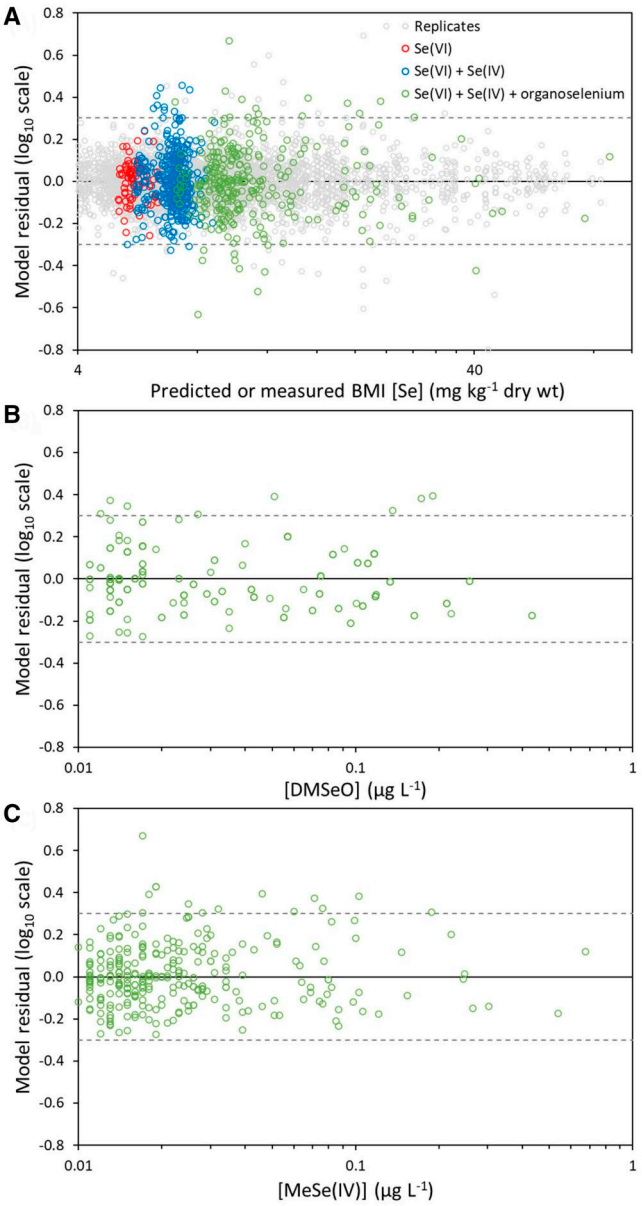

Figure 4. Residuals of the final bioaccumulation model relative to (A) model predictions, (B) dimethylselenoxide (DMSeO) concentration, and (C) methylseleninic acid concentration ([MeSe(IV)]). Solid horizontal line is perfect agreement between observed and predicted benthic macroinvertebrate (BMI) Se concentrations. Dashed horizontal lines indicate plus or minus a factor of 2 from perfect agreement. Se(VI) = selenate; Se(IV) = selenite. Variability of replicate observed BMI Se concentrations shown in (A) for comparison.

model applied to the oxyanion-only dataset, with 80% of observations within a factor of 1.5 of model predictions and 94% within a factor of 2 (Figure 5).

It is difficult to evaluate the organoselenium EF estimates derived above relative to published data because few studies have tested bioaccumulation of species other than selenite and selenate, largely because knowledge of organoselenium in aquatic environments is limited (but cf Ponton & Hare, 2013). Organoselenium species are connected to the metabolism of SeCys and SeMet, which are the two main organic forms of Se that occur within organisms (Janz et al., 2014; Rigby et al., 2014). Studies of the biogeochemical metabolism of these organoselenides in aquatic environments are rare and metabolites of

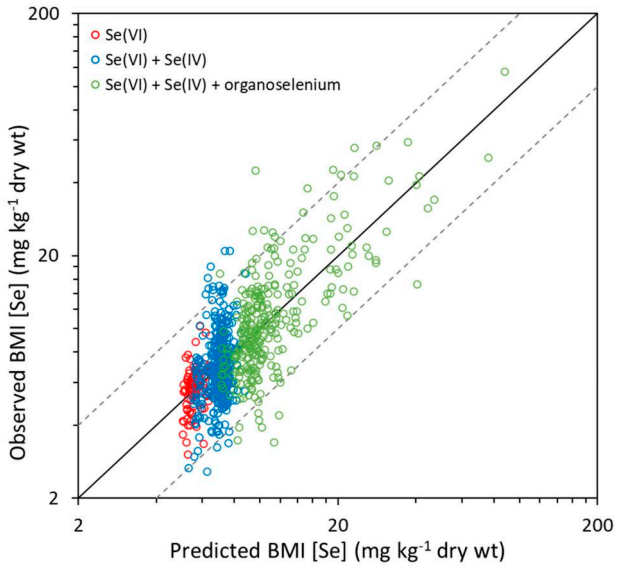

Figure 5. Overall performance of the final bioaccumulation model for sites with differing speciation. Solid diagonal line is perfect agreement between observed and predicted benthic macroinvertebrate (BMI) selenium (Se) concentrations. Dashed diagonal lines indicate plus or minus a factor of 2 from perfect agreement. Se(VI) = selenate; Se(IV) = selenite.

selenoamino acids have not previously been considered in toxicity or bioavailability studies. Until recently, studies of Se in natural waters or in experiments either have not reported organoselenium species or have reported them as a bulk entity inferred as the difference between aqueous Se and measured Se oxyanions. With recent advances in analytical capabilities, some specific organoselenium species can be separated (e.g., LeBlanc & Wallschläger, 2016; data reported herein). It is now apparent that SeMet and SeCys are themselves rarely if ever detected in natural waters, including our study area (LeBlanc & Wallschläger, 2016; data reported herein). Selenoamino acids are expected to be released to the water column when organisms die or are consumed but appear to be unstable and rapidly degrade into the methylated species measured in our study.

The few studies that have measured uptake of organoselenium all have faced a common set of challenges. First, experiments with aquatic organisms typically assume that the nominally introduced form of Se remains stable throughout the experiment, whereas it is clear that at least some forms are unstable in freshwaters and in experiments. Conley et al. (2013) showed a gradual conversion of selenate to selenite over a 10-day static exposure of periphyton. They did not analyze for organoselenium, but some transformation and release of biological metabolites could explain why that study (and some others, e.g., the field-collected microplankton exposures of Ponton et al., 2018) attributed relatively higher EFs to selenite than others (e.g., Besser et al., 1993; Conley et al., 2009, 2011, 2013; Riedel & Cole, 2001).

In addition, experiments have not studied relevant forms of Se. Nearly all studies to date have measured uptake of SeMet. Estimates of SeMet bioavailability range from five- to 100-fold greater than selenite (Kiffney & Knight, 1990; Riedel et al., 1991; Besser et al., 1993; Fournier et al., 2006). Baines et al. (2001) used a different approach, obtaining a mixture of organoselenium by lysing algal cells grown in a medium spiked with radiolabelled Se and reported that bioaccumulation of Se from this lysate was similar to selenite. However, the lysates were an uncharacterized mixture of organic and inorganic species. It is unclear from these studies how bioavailability of metabolites of selenoamino acids compares with their parent forms.

Another challenge in laboratory studies is depletion of bioavailable species from media. Depletion of Se from media has been noted to be especially rapid with organic Se species (e.g., Besser et al., 1993; Kiffney & Knight, 1990), perhaps because of their greater bioavailability or perhaps because of the tendency for some fraction to volatilize on conversion to DMSe or DMDSe. Shorter term studies of uptake rates (e.g., Baines et al., 2001; Fournier et al., 2006; Riedel et al., 1991) may provide more reliable estimates of bioavailability but must be used to estimate *EF* from uptake kinetics, rather than directly as a concentration ratio. Riedel et al. (1991) and Fournier et al. (2006) found SeMet bioavailability expressed as uptake rates to be five- to 50-fold greater than selenite.

Finally, studies of Se uptake by algae are often conducted with cultures in an exponential growth phase. Differences in growth rates among treatments (e.g., Kiffney & Knight, 1990), experiments, or species of algae (e.g., Baines et al., 2001) can influence absolute values of EF and affect interpretations of relative EF.

Summary

This extensive and detailed simultaneous characterization of Se speciation and BMI [Se] across a range of lotic conditions in the Elk Valley watershed provided a unique opportunity to quantify the contribution of speciation in the Se exposure of a food web as well as identifying sources of the most bioavailable species. The number of sampling events is exceptionally large and covers a nearly 100-fold range in concentrations of multiple Se species. Covariances that can limit statistical interpretations from a single watershed are reduced here by the wide range of lotic conditions sampled.

The observational dataset we were able to generate also allowed us to address some challenges faced by previous experimental studies with laboratory cultures and field mesocosms. Notably, the lotic habitats we studied have aqueous speciation that is continually replenished from upstream areas. The organoselenium species we detected are highly labile, which would make them difficult to study were they not being continually generated by biological processes upstream of our study sites. The flow-through nature of our sites prevents depletion of aqueous concentrations and reduces the potential for in situ conversion and recycling of reduced species that occurs in lentic areas (and that could occur in nonflowing laboratory or field experiments). Variation in speciation with the seasonal development and senescence of biological communities in mine ponds could be a source of residual variance in the model (Brandt et al., 2021). However, it appeared that changes on the time scale of weeks to months may be slow enough that BMI [Se] can remain near steady state much of the time (DeForest et al., 2016).

A strength of our analysis was relying on BMI [Se] to quantify bioaccumulation, avoiding the analytical, logistical, and bioavailability issues (Brandt et al., 2021) associated with attempting to directly measure [Se] transfer to consumers from basal organisms. Our approach combined algal uptake and trophic transfer to invertebrates into a single model step, effectively treating BMIs as a "black box". This approach follows conventional wisdom that the algal uptake step (which is directly influenced by aqueous speciation) is the largest and most variable part of the bioaccumulation process, and that trophic transfer (which could

be influenced by BMI composition but not directly by aqueous speciation) is less variable (Presser & Luoma, 2010).

A portion of unexplained variance in our dataset is likely related to kinetics, particularly during times of year when aqueous speciation changes more rapidly than BMI [Se] can reach steady state. Other sources of residual variance could include within-site variation in speciation related to microhabitats and taxonomic differences in bioaccumulation related to physiology, use of different microhabitats, or consumption of authochthonous versus allochthonous resources. We attempted to minimize these factors by focusing our analysis on nondepositional lotic sites and removing a small number of depositional sites that violated this assumption of our analysis. As shown in Figure S4, depositional characteristics reduce the explanatory power of overlying water speciation. It is likely that bioaccumulation in lentic environments would not be well predicted by our model unless speciation could be measured in relevant microenvironments such as porewater (e.g., Martin et al., 2011, 2018).

Despite several simplifications of reality in our modeling approach, aqueous speciation alone was able to explain more than half of the variance in BMI [Se] ($r^2_{corr} = 0.52$) across a wide range of concentrations, speciation, and other characteristics that varied over multiple years at 137 study sites. Our analysis showed that organoselenium species at parts-per-trillion levels can dominate BMI [Se] due to their high bioavailability compared with inorganic species. These and other products of Se metabolism may play a larger role in observed patterns of bioaccumulation than previously recognized, in both lentic and lotic environments. This finding highlights the importance of understanding and managing the biological processes that generate these species to manage Se risk.

Supplementary material

Supplementary material is available online at *Environmental Toxicology and Chemistry*.

Data availability

Data, associated metadata, and calculation tools are available in the supporting information and from the corresponding author (adrian.debruyn@outlook.com).

Author contributions

Adrian de Bruyn (Conceptualization, Formal analysis, Investigation, Methodology, Writing—original draft, Writing—review & editing) Cybele Heddle (Data curation, Project administration) Jennifer Ings (Investigation) Hakan Gurleyuk (Investigation) Kevin Brix (Conceptualization, Writing—review & editing) Sam Luoma (Conceptualization, Writing—review & editing) Mariah Arnold (Funding acquisition, Project administration, Writing—review & editing)

Funding

Funding was provided by Teck Coal Limited.

Conflicts of interest

The authors declare no conflict of interest.

Disclaimer

The peer review for this article was managed by the Editorial Board without the involvement of Kevin V. Brix.

Acknowledgments

This study was conducted on Qukin ?amak?is, the traditional and unceded homelands of the Ktunaxa Nation.

References

Adams, W. J., Brix, K. V., Edwards, M., Tear, L. M., DeForest, D. K., & Fairbrother, A. (2003). Analysis of field and laboratory data to derive selenium toxicity thresholds for birds. *Environmental Toxicology and Chemistry*, *22*, 2020–2029.

Ashby, L. J., Mill, K. E. C., Arnold, M. C., Van Geest, J. L., & de Bruyn, A. M. H. (2023). Analysis of selenium in fish tissue: an interlaboratory study on weight constraints. *Environmental Toxicology and Chemistry*, *42*, 2119–2129.

Bailey, F. C., Knight, A. W., Ogle, R. S., & Klaine, S. J. (1995). Effect of sulfate level on selenium uptake by *Ruppia maritima*. *Chemosphere*, *30*, 579–591.

Baines, S. B., Fisher, N. S., Doblin, M. A., & Cutter, G. A. (2001). Uptake of dissolved organic selenides by marine phytoplankton. *Limnology and Oceanography*, *46*, 1936–1944.

Beckon, W. N. (2016). A method for improving predictive modeling by taking into account lag time: Example of selenium bioaccumulation in a flowing system. *Aquatic Toxicology (Amsterdam, Netherlands)*, *176*, 172–180.

Besser, J. M., Canfield, T. J., & La Point, T. W. (1993). Bioaccumulation of organic and inorganic selenium in a laboratory food chain. *Environmental Toxicology and Chemistry*, *12*, 57–72.

Brandt, J. E., Roberts, J. J., Stricker, C. A., Rogers, H. A., Nease, P., & Schmidt, T. S. (2021). Temporal influences on selenium partitioning, trophic transfer, and exposure in a major U.S. river. *Environmental Science & Technology*, *55*, 3645–3656.

Brix, K. V., Toll, J. E., Tear, L. M., DeForest, D. K., & Adams, W. J. (2005). Setting site-specific water-quality standards by using tissue residue thresholds and bioaccumulation data. Part 2. Calculating site-specific selenium water-quality standards for protecting fish and birds. *Environmental Toxicology and Chemistry*, *24*, 231–237.

Conley, J. M., Funk, D. H., & Buchwalter, D. B. (2009). Selenium bioaccumulation and maternal transfer in the mayfly *Centroptilum triangulifer* in a life-cycle, periphyton-biofilm trophic assay. *Environmental Science & Technology*, *43*, 7952–7957.

Conley, J. M., Funk, D. H., Cariello, N. J., & Buchwalter, D. B. (2011). Food rationing affects dietary selenium bioaccumulation and life cycle performance in the mayfly *Centroptilum triangulifer*. *Ecotoxicology*, *20*, 1840–1851.

Conley, J. M., Funk, D. H., Hesterberg, D. H., Hsu, L.-C., Kan, J., Liu, Y.-T., & Buchwalter, D. B. (2013). Bioconcentration and biotransformation of selenite versus selenate exposed periphyton and subsequent toxicity to the mayfly *Centroptilum triangulifer*. *Environmental Science & Technology*, *47*, 7965–7973.

Cooke, T. D., & Bruland, K. W. (1987). Aquatic chemistry of selenium: Evidence of biomethylation. *Environmental Science & Technology*, *21*, 1214–1219.

Cutter, G. A., & Bruland, K. W. (1984). The marine biogeochemistry of selenium: A re-evaluation. *Limnology & Oceanography*, *29*, 1179–1192.

Cutter, G. A., & San Diego-McGlone, M. L. C. (1990). Temporal variability of selenium fluxes in San Francisco Bay. *Science of the Total Environment*, 97-98, 235–250.

DeForest, D. K., Brix, K. V., Elphick, J. R., Rickwood, C. J., deBruyn, A. M. H., Tear, L. M., Gilron, G., Hughes, S. A., & Adams, W. J. (2017). Lentic, lotic, and sulfate-dependent waterborne selenium screening guidelines for freshwater systems. *Environmental Toxicology and Chemistry*, 36, 2503–2513.

DeForest, D. K., Pargee, S., Claytor, C., Canton, S. P., & Brix, K. V. (2016). Biokinetic food chain modeling of waterborne selenium pulses into aquatic food chains: Implications for water quality criteria. *Integrated Environmental Assessment and Management*, 12, 230–246.

Dungan, R. S., & Frankenberger Jr., W. T. (1999). Microbial transformations of selenium and the bioremediation of seleniferous environments. *Bioremediation Journal*, 3, 171–188.

Environment Canada. (2012). Canadian aquatic biomonitoring network: Field manual for wadeable streams. https://publications.gc.ca/site/eng/422979/publication.html

Eswayah, A. S., Smith, T. J., & Gardiner, P. H. E. (2016). Microbial transformations of selenium species of relevance to bioremediation. *Applied and Environmental Microbiology*, 82, 4848–4859.

Faust, S. D., & Aly, O. M. (1981). *Chemistry of Natural Waters*. Ann Arbor Science.

Fournier, E., Adam, C., Massabuau, J. C., & Garnier-Laplace, J. (2006). Selenium bioaccumulation in *Chlamydomonas reinhardtii* and subsequent transfer to *Corbicula fluminea*: Role of selenium speciation and bivalve ventilation. *Environmental Toxicology and Chemistry*, 25, 2692–2699.

Goeger, D. E., & Ganther, H. E. (1994). Oxidation of dimethylselenide to dimethylselenoxide by microsomes from rat liver and lung and by flavin-containing monooxygenase from pig liver. *Archives of Biochemistry and Biophysics*, 310, 448–451.

Hitchcock, A. P., Dynes, J. J., Lawrence, J. R., Obst, M., Swerhone, G. D. W., Korber, D. R., & Leppard, G. G. (2009). Soft X-ray spectromicroscopy of nickel sorption in a natural river biofilm. *Geobiology*, 7, 432–453.

Hu, M., Yang, Y., Martin, J., Yin, K., & Harrison, P. J. (1997). Preferential uptake of SeIV over SeVI and the production of dissolved organic Se by marine phytoplankton. *Marine Environmental Research*, 44, 225–231.

Jain, V. K. (2017). An overview of organoselenium chemistry: From fundamentals to synthesis. In V. K. Jain & K. I. Priyadarsini (Eds.), *Organoselenium Compounds in Biology and Medicine: Synthesis, Biological and Therapeutic Treatments* (pp. 1–33). Royal Society of Chemistry. https://doi.org/10.1039/9781788011907

Janz, D. M., DeForest, D. K., Brooks, M. L., Chapman, P. M., Gilron, G., Hoff, D., Hopkins, W. A., McIntyre, D. O., Mebane, C. A., Palace, V. P., Skorupa, J. P., & Wayland, M. (2010). Selenium toxicity to aquatic organisms. In: P. M. Chapman, W. J. Adams, M. L. Brooks, C. G. Delos, S. N. Luoma, W. A. Maher, H. M. Ohlendorf, T. S. Presser, & D. P. Shaw (Eds.), *Ecological assessment of selenium in the aquatic environment* (pp. 141–231). CRC Press. https://doi.org/10.1201/EBK1439826775

Janz, D. M., Liber, K., Pickering, I. J., Wiramanaden, C. I. E., Weech, S. A., Gallego-Gallegos, M., Driessnack, M. J., Franz, E. D., Goertzen, M. M., Phibbs, J., Tse, J. J., Himbeault, K. T., Robertson, E. L., Burnett-Seidel, C., England, K., & Genty, A. (2014). Integrative assessment of selenium speciation, biogeochemistry, and distribution in a northern coldwater ecosystem. *Integrated Environmental Assessment and Management*, 10, 543–554.

Kiffney, P., & Knight, A. (1990). The toxicity and bioaccumulation of selenate, selenite and seleno-L-methionine in the cyanobacterium *Anabaena flos-aquae*. *Archives of Environmental Contamination & Toxicology*, 19, 488–494.

Kuchapski, K. A., & Rasmussen, J. B. (2015). Food chain transfer and exposure effects of selenium in salmonid fish communities in two watersheds in the Canadian Rocky Mountains. *Canadian Journal of Fisheries and Aquatic Sciences*, 72, 955–967.

LeBlanc, K. L., & Wallschläger, D. (2016). Production and release of selenomethionine and related organic selenium species by microorganisms in natural and industrial waters. *Environmental Science & Technology*, 50, 6164–6171.

Lo, B. P., Elphick, J. R., Bailey, H. C., Baker, J. A., & Kennedy, C. J. (2015). The effect of sulphate on selenate bioaccumulation in two freshwater primary producers: A duckweed, *Lemna minor*, and a green alga, *Pseudokirchneriella subcapitata*. *Environmental Toxicology and Chemistry*, 34, 2841–2845.

Lunøe, K., Skov, S., Gabel-Jensen, C., Stürup, S., & Gammelgaard, B. (2010). A method for analysis of dimethyl selenide and dimethyl diselenide by LC-ICP-DRC-MS. *Analytical and Bioanalytical Chemistry*, 398, 3081–3086.

Luoma, S. N., & Rainbow, P. S. (2008). Selenium: Dietary exposure, trophic transfer and food web effects. In S. N. Luoma & P. S. Rainbow (Eds.), *Metal contamination in aquatic environments: Science and lateral management* (pp. 327–351). Cambridge University Press. https://doi.org/10.1111/j.1095-8649.2009.02440_4.x

Maher, W., Roach, A., Doblin, M., Fan, T., Foster, S., Garrett, R., Möller, G., Oram, L., & Wallschläger, D. (2010). Environmental sources, speciation, and partitioning of selenium. In: P. M. Chapman, W. J. Adams, M. L. Brooks, C. G. Delos, S. N. Luoma, W. A. Maher, H. M. Ohlendorf, T. S. Presser, & D. P. Shaw (Eds.), *Ecological assessment of selenium in the aquatic environment* (pp. 47–92). CRC Press. https://doi.org/10.1201/EBK1439826775

Martin, A., Simpson, S., Fawcett, S., Wiramanaden, C. I. E., Pickering, I. J., Belzile, N., Chen, Y.-W., London, J., & Wallschläger, D. (2011). Biogeochemical mechanisms of selenium exchange between water and sediments in two contrasting lentic environments. *Environmental Science & Technology*, 45, 2605–2612.

Martin, A. J., Fraser, C., Simpson, S., Belzile, N., Chen, Y. W., London, J., & Wallschläger, D. (2018). Hydrological and biogeochemical controls governing the speciation and accumulation of selenium in a wetland influenced by mine drainage. *Environmental Toxicology and Chemistry*, 37, 1824–1838.

Martin, A. J., Kuang, C., & Wallschlager, D. (2022). Expansion of the conceptual model for the accumulation of selenium in lentic food chains to include redox-controlled generation and diffusion of selenite and dissolved organo-selenium compounds. *Environmental Toxicology and Chemistry*, 41, 2859–2869.

Milne, J. B (1998). The uptake and metabolism of inorganic selenium species. In: W.T. Frankenberger Jr., & R.A. Engberg (Eds.), *Environmental chemistry of selenium*. (pp. 459–478). CRC Press. https://doi.org/10.1201/9781482269949

Neumann, P. M., De Souza, M. P., Pickering, I. J., & Terry, N. (2003). Rapid microalgal metabolism of selenate to volatile dimethylselenide. *Plant, Cell & Environment*, 26, 897–905.

Orr, P. L., Guiguer, K. R., & Russel, C. K. (2006). Food chain transfer of selenium in lentic and lotic habitats of a western Canadian watershed. *Ecotoxicology and Environmental Safety*, 63, 175–188.

Orr, P. L., Wiramanaden, C. I., Paine, M. D., Franklin, W., & Fraser, C. (2012). Food chain model based on field data to predict westslope cutthroat trout (*Oncorhynchus clarkii lewisi*) ovary selenium concentrations from water selenium concentrations in the Elk Valley, British Columbia. *Environmental Toxicology and Chemistry*, 31, 672–680.

Ponton, D. E., & Hare, L. (2013). Relating selenium concentrations in a planktivore to selenium speciation in lakewater. *Environmental Pollution*, *176*, 254–260.

Ponton, D. E., Fortin, C., & Hare, L. (2018). Organic selenium, selenate, and selenite accumulation by lake plankton and the alga *Chlamydomonas reinhardtii* at different pH and sulfate concentrations. *Environmental Toxicology and Chemistry*, *37*, 2112–2122.

Ponton, D. E., Graves, S. D., Fortin, C., Janz, D., Amyot, M., & Schiavon, M. (2020). Selenium interactions with algae: Chemical processes at biological uptake sites, bioaccumulation, and intracellular metabolism. *Plants*, *9*, 528.

Presser, T. S., & Luoma, S. N. (2010). A methodology for ecosystem-scale modeling of selenium. *Integrated Environmental Assessment and Management*, *6*, 685–710.

Riedel, G. F., & Cole, L. (2001). Transfer of selenium in the benthic food web. In *Selenium cycling and impact in aquatic ecosystems: Defining trophic transfer and waterborne exposure pathways* (pp. 3–21). Electric Power Research Institute. https://www.epri.com/research/products/000000000001005217

Riedel, G. F., Ferrier, D. P., & Sanders, J. G. (1991). Uptake of selenium by fresh-water phytoplankton. *Water, Air, and Soil Pollution*, *57-58*, 23–30.

Riedel, G. F., & Sanders, J. G. (1996). The influence of pH and media composition on the uptake of inorganic selenium by *Chlamydomonas reinhardtii*. *Environmental Toxicology and Chemistry*, *15*, 1577–1583.

Rigby, M. C., Lemly, A. D., & Gerads, R. (2014). Fish toxicity testing with selenomethionine spiked feed—What's the real question being asked? *Environmental Science, Processes & Impacts*, *16*, 511–517.

Rosenfeld, C. E., Sabuda, M. C., Hinkle, M. A. G., James, B. R., & Santelli, C. M. (2020). A fungal-mediated cryptic selenium cycle linked to manganese biogeochemistry. *Environmental Science & Technology*, *54*, 3570–3580.

Simmons, D. B. D., & Wallschläger, D. (2005). A critical review of the biogeochemistry and ecotoxicology of selenium in lotic and lentic environments. *Environmental Toxicology and Chemistry*, *24*, 1331–1343.

Simmons, D. B. D., & Wallschläger, D. (2011). Release of reduced inorganic selenium species into waters by the green fresh water algae *Chlorella vulgaris*. *Environmental Science & Technology*, *45*, 2165–2171.

Stewart, A. R., Grosell, M., Buchwalter, D., Fisher, N., Luoma, S., Matthews, T., Orr, P., & Wang, W.-X. (2010). Bioaccumulation and trophic transfer of selenium. In: P. M. Chapman, W. J. Adams, M. L. Brooks, C. G. Delos, S. N. Luoma, W. A. Maher, H. M. Ohlendorf, T. S. Presser, & D. P. Shaw (Eds.), *Ecological assessment of selenium in the aquatic environment* (pp. 93–140). CRC Press. https://doi.org/10.1201/EBK1439826775

Swift, M. C. (2002). Stream ecosystem response to, and recovery from, experimental exposure to selenium. *Journal of Aquatic Ecosystem Stress and Recovery*, *9*, 159–184.

Vriens, B., Behra, R., Voegelin, A., Zupanic, A., & Winkel, L. H. E. (2016). Selenium uptake and methylation by the microalga *Chlamydomonas reinhardtii*. *Environmental Science & Technology*, *50*, 711–720.

Wallschläger, D., & Bloom, N. S. (2001). Determination of selenite, selenate and selenocyanate in waters by ion chromatography-hydride generation-atomic fluorescence spectrometry (IC-HG-AFS). *Journal of Analytical Atomic Spectrometry*, *16*, 1322–1328.

Wallschläger, D., & Feldmann, J. (2010). Formation, occurrence, significance, and analysis of organoselenium and organotellurium compounds in the environment. *Metal Ions in Life Sciences*, *7*, 319–364.

Wang, B., & Burau, R. G. (1995). Oxidation of dimethylselenide by delta-MnO2: oxidation product and factors affecting oxidation rate. *Environmental Science & Technology*, *29*, 1504–1510.

Williams, M. J., Ogle, R. S., Knight, A. W., & Burau, R. G. (1994). Effects of sulfate on selenate uptake and toxicity in the green alga *Selenastrum capricornutum*. *Archives of Environmental Contamination & Toxicology*, *27*, 449–453.

Winkel, L., Feldmann, J., & Meharg, A. A. (2010). Quantitative and qualitative trapping of volatile methylated selenium species entrained through nitric acid. *Environmental Science & Technology*, *44*, 382–387.

Zhang, H., Feng, X., & Larssen, T. (2014). Selenium speciation, distribution, and transport in a river catchment affected by mercury mining and smelting in Wanshan, China. *Applied Geochemistry*, *40*, 1–10.

Zhang, Y., & Frankenberger Jr., W. T. (2000). Formation of dimethylselenonium compounds in soil. *Environmental Science & Technology*, *34*, 776–783.

Zhang, Y. Q., Frankenberger Jr., W. T., & Moore, J. N. (1999). Effect of soil moisture on dimethylselenide transport and transformation to nonvolatile selenium. *Environmental Science & Technology*, *33*, 3415–3420.

Environmental Toxicology and Chemistry, 2025, 44, 363–374
https://doi.org/10.1093/etojnl/vgae036
Original Article